Advanced Remote Control Using Gesture-Based Teleoperation and Naked-Eye 3D Display

Chung-Chun Wang and Cheng-Wei Chen, *Member, RST*

***Abstract*—The design of the remote control interface offers the surgeon a better, intuitive way to perform robot-assisted minimally invasive surgeries. Among various control interfaces, the gesture-based controller provides increased mobility and convenience for surgeons as if they were operating with their bare hands. However, arm fatigue issues have been reported as the surgeons have to hold their arms in an unsupported manner such that the surgical instrument is steadily located at the target position. We propose a teleoperation interface based on a novel motion mapping to solve this problem. Surgeons wave their arms or palms to move or insert the teleoperated instrument. In addition, naked-eye 3D visualization is integrated with the control interface. Surgeons are provided with adequate depth information but are free from discomfort symptoms caused by head-mounted devices. The proposed framework is demonstrated on the LapaRobot, a robotic surgical system designed for telementoring and training in laparoscopic surgery. The experimental results indicate that the proposed interface reduces users' burden and achieves more precise master path planning.**

***Index Terms*—Teleoperation, Gesture-based control, Arm fatigue, Hand-robot motion mapping, Motion scaling, Naked-eye 3D visualization, Autostereoscopic display**

I. Introduction

TELEROBOTICS enables robot manipulation without distance restriction and transfers human manipulation skills and dexterity to a remote workplace [1]. Based on these benefits, in the medical field, telerobotics has been applied in robot-assisted surgery. Robot-assisted surgery aims to cope with human limitations that surgeons confront in minimally invasive surgery. It has been successfully applied to cardiothoracic surgery [2], colorectal surgery [3], gynecology [4], and many other type of general surgery.

Though the telerobotic surgical system brings mobility and accuracy to clinical procedures, surgeons report that most touch-based control interfaces, e.g., joysticks, limit the naturalness and range of motion [5]. Using these traditional touch-based interfaces, users need significant training to get familiar with the coordinate mapping between the master device and the surgical robot [5]. Nonetheless, touchless interfaces allow for increased mobility and convenience for surgeons as they were operating with their bare hands. Among them, gesture-based interfaces, such as Microsoft Kinect [6] and Leap Motion Controller [5], are commonly used for hand detection and gesture recognition in teleoperation systems, in which the surgical instrument' motion replicates the user' hand movement during the operation.

When using a gesture-based controller, surgeons must also hold their arms in unsupported positions to locate the surgical instrument at target positions. Severe fatigue problems after hanging their arms for a while have been reported [5]. This issue has also been reproduced in our teleoperating surgical system, which consists of a laparoscopic training robot developed by the UCLA team [7] and a hand tracking module. In our preliminary experiment, 7 of 10 participants reported hand and arm fatigue problems that need to be overcome.

Besides, real-time visual feedback also plays an essential role in the telerobotic surgical system. In some applications, surgeons are provided with 2D vision captured by an endoscope [8]. Insufficient depth information causes longer surgical task completion time and lower surgical precision. Until now, in the medical field, most of the 3D displays are head-mounted. Early studies indicate that this kind of device causes 60% of study participants symptoms of eye strain or headache [9].

In this study, a novel robot-hand motion mapping is proposed to alleviate the arm fatigue problem when applying a touchless control interface. By placing the user's elbow on the table during the operation, the novel mapping does not require the user to hang or hold their arm during the operation. This design not only solves the arm fatigue problem but also prevents the user's hand from leaving the sensor range and, therefore, avoids losing hand tracking. In addition, an autostereoscopic display, which enables naked-eye 3D perception, is integrated with our system to reduce surgeons' discomfort caused by the conventional head-mounted display.

The remainder of the article is organized as follows: the main components integrated for the teleoperating surgical system are described in Section II; the proposed hand-robot motion mapping is elaborated in Section III; In Section IV, participants are asked to perform pre-clinical tasks using the proposed control interface. The efficacy of proposed hand-robot motion mapping and real-time 3D surgical vision in task performance is evaluated; the concluding remarks are given in Section V.

II. System Description

In this section, the teleoperating surgical system developed in this study will be briefly introduced. It consists of a robotic surgical manipulator, a hand gesture tracker, a stereo camera, and a 3D hologram display. The overall system architecture along with the proposed advanced remote control interface is as illustrated in Fig. 1.

Chung-Chun Wang and Cheng-Wei Chen are with the Department of Electrical Engineering, National Taiwan University, Taipei, Taiwan.

This work was supported in part by the National Science and Technology Council in Taiwan (Young Scholar Fellowship MOST 111-2636-E-002-028).
Corresponding author: Cheng-Wei Chen (email: cwchenee@ntu.edu.tw)

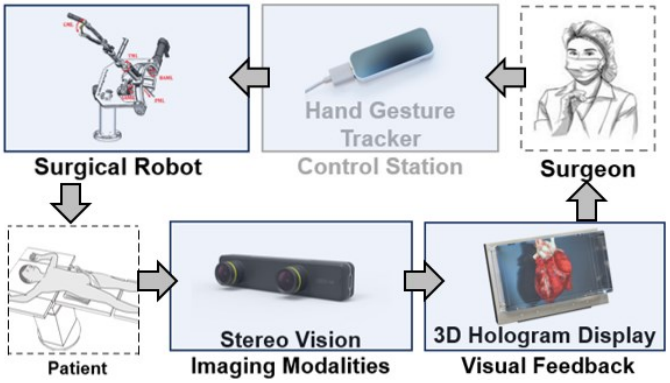

Fig. 1. System architecture of the teleoperating surgical system with the proposed advanced remote control interface. The 3D visual feedback captured by a stereo camera is display to the surgeon through a hologram display. The surgeon uses hand gesture to control the motion of the robotic manipulator.

A. Microsurgical Robot – LapaRobot

The LapaRobot (Fig. 2), a robotic surgical system designed for telementoring and training in laparoscopic surgery [7], is applied as the robotic manipulator on the slave side. This robotic manipulator is composed of 5 degrees of freedom, including the spherical remote-center-of-motion (RCM) mechanism, tool translation mechanism, and instrument grasping mechanism. The pitch ($-60^\circ \leq \varphi \leq 60^\circ$) arc and roll ($-40^\circ \leq \phi \leq 40^\circ$) arc guide the surgical instrument about the RCM in the spherical mechanism. To fulfill the requirements of laparoscopic surgical training, the spherical arcs in the mechanism maintain an RCM within 0.5 mm. Among them, the primary slider maintains concentricity of the tool mechanism with the radial surfaces of the arc while the lower slider is forced to move within the secondary arc. Tool translation in the mechanism is actuated by a rack and a gear, providing smooth parallel actuation for 60 mm along the tool insertion axis. Tool rotation is realized through two gears and is able to rotate around 260°. Besides, the robot is capable of mounting commonly used laparoscopic tools. All the design mentioned above makes LapaRobot the right choice of our system.

To improve the stability of our teleoperation system and reduce the wear and tear of our robot mechanism, we set up several system characteristics. These characteristics will be introduced below. First, we apply a moving average filter to our robot command in case sensor noises disturb the system. Every input of robot command would be added to the sum of the previous seven robot commands and averaged. By doing so, interferences from unstable sensor values during teleoperation would be eliminated. Second, maximal increment rates are set to protect motors in the robot. When the user's hand moves too fast, large deviations appear in the value of the robot command. The motors would follow the commands based on the maximal increment rates, reach the target position steps by steps, and avoid the robot from being broken. Users can directly modify the maximal increment rates of every joint motor through LabVIEW interface of our system. Command saturations are also implemented in our system, limiting the motors' revolution and forbidding the robot to run out of its working range.

Fig. 2. LapaRobot [7] installed with a forcep for executing teleoperated surgical tasks.

Fig. 3. Advanced remote control interface consists of a 3D hologram display (Looking Glass 8.9", Looking Glass Factory, Brooklyn, NY) and a hand gesture tracker (Leap Motion Controller, Ultraleap, Mountain View, CA).

B. Naked-Eye 3D Display

Human perceptual cues are needed to facilitate surgical performance. A 3D vision of the surgical site provides adequate depth information between surgical tools and patients' bodies. Being able to render 3D content without leading to users' discomfort, a naked-eye 3D hologram display (Looking Glass 8.9", Looking Glass Factory, Brooklyn, NY) is integrated into our system, as shown in Fig. 3.

The hologram display is used to render the real-time 3D point cloud of patient anatomy captured from the stereo camera (ZED mini, Stereolabs, San Francisco, CA). Without any eye-tracking or headsets, the autostereoscopic display not only mitigates surgeons' discomfort but allows multiple viewers to see the 3D image at the same time. This characteristic hits the spot since surgeons often need to discuss or cooperate with assistants during the operation. If all of them are allowed to see the point cloud from different perspectives simultaneously, it may greatly improve surgical efficiency and performance. Apart from the large field of view of 50 degrees, this display also possesses a high refresh rate. It reduces input lag in the teleoperation system.

C. Gesture-Based Control Interface

A hand gesture tracker (Leap Motion Controller, Ultraleap, Mountain View, CA) is selected as the master device to control the slave robotic manipualtor. The Leap Motion Controller (LMC) is an optical hand tracking module capturing the movement and gesture of user's hands. We apply LMC in our system due to several reasons. First of all, its small design makes it portable. Next, its high data processing rate makes it suitable for real-time control. Besides, Ultraleap Tracking SDK and its Unity modules make it easy to apply hand data into our system. The device is composed of two cameras and three infrared LEDs. Outside the visible light spectrum, the infrared light sources prevent hand detection from being disturbed by ambient environmental lighting. With two cameras spaced 40 millimeters apart, LMC computes the data of hand objects and performs 3D reconstruction through stereo triangulation. Then, the hand tracking algorithms provided by Ultraleap match the 3D data and interpret it with digital content.

III. Novel Hand-Robot Motion Mapping

In this section, a novel motion mapping between gesture and surgical instrument is proposed to alleviate the arm fatigue problem.

A. Design Concept

To avoid hand and arm fatigue problems, the only way without applying any auxiliary devices is to rest the user's elbow on the table while performing tasks. The two rotational degrees of freedom of the user's wrist position, as the elbow is served as the pivot point, are mapped to the pitch and roll angles of the LapaRobot. The comparisons of the conventional and the proposed motion mapping are illustrated in Fig. 4. Due to restricted active range of hand motion, the user's wrist position is projected onto xz-plane and sent as the reference command to the slave robot in our design.

On the other hand, to cope with the limited y-axis motion range of the user's hand, we replace the wrist position y-axis coordinate with the wrist angle, i.e., the angle value between y-axis and the vector from wrist position coordinate to pinky fingertip position as shown in Fig. 4. As a result, users insert the surgical tool by waving down their palms. This design avoids the users' tool insertion performance being affected by their finger positions, which may have unconscious movement during the operation.

B. Initialization Procedure

While using the proposed motion mapping, participants with longer arms indicate that 1:1 hand-robot mapping causes overspeed operation of the surgical tool. If participants with longer arms want to perform delicate operations, they need to hold their arms in a small range, which is backbreaking. Hence, hand-robot motion scaling based on the length of the user's arm is necessary. Though we can directly measure the user's arm length, it is not practical if the system is used for medical education and hundreds of users. Measuring the user's arm length and saving the data into the system manually is a waste of time.

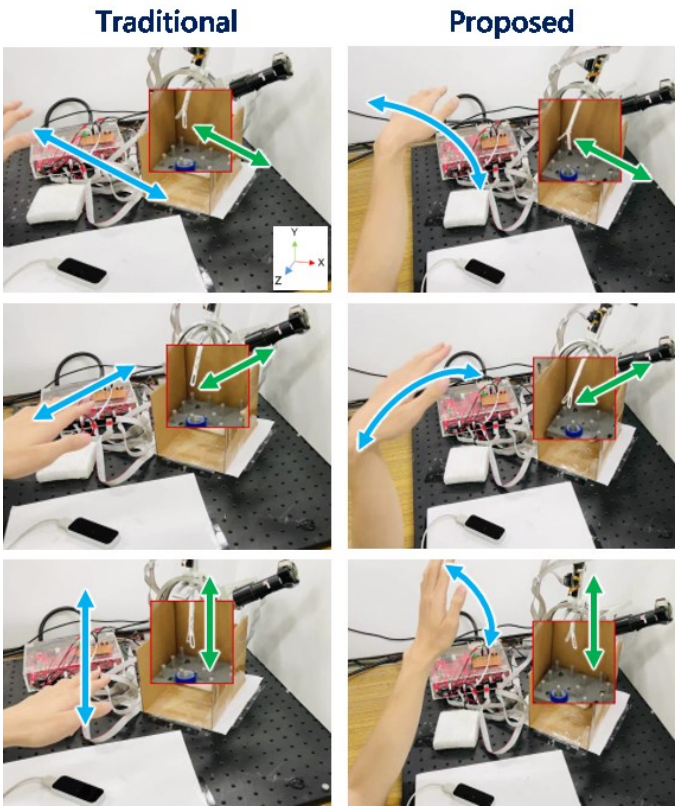

Fig. 4. Traditional and proposed motion mapping between hand gestures (blue) and teleoperated movements (green).

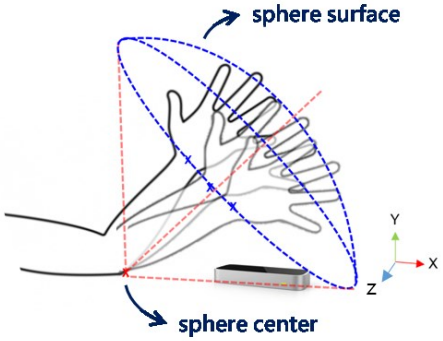

Fig. 5. Estimation of the user's arm length by fitting a sphere to data points collected from the hand gesture tracker.

A method to estimate the user's arm length automatically is developed in this study. We found that while the user waves his/her arm with his/her elbow fixed on the table, his/her wrist's trajectory draws over a sphere surface as shown in Fig. 5. The center of the sphere is located on the user's elbow. Therefore, we apply the Least-Square Sphere Fitting method [10], and the radius of the sphere is the user's arm length.

In this initialization procedure, the user needs to wave his/her arm with a fixed elbow position for 10 seconds. The Unity project, running in 50 fps, would automatically save 500 points position as data points $[x_n \;\; y_n \;\; z_n]$. After applying the Least-Square Sphere Fitting method, we can obtain the sphere center and the length of user's arm L_{arm}. This process also helps users get used to the system and master the rule of manipulation.

C. Motion Mapping and Scaling

We adopt velocity scaling and user-based scaling in our hand-robot motion mapping. The velocity scaling factor and user-based scaling factor are multiplied together. The penalty of these two factors works and provides a higher level of intuitiveness to users. Based on the user's arm length, the ultimate scaling factor varies with the master velocity. If the user has a longer arm, the scaling factor remains small no matter how fast he/she waves his/her arm, and vice versa.

In summary, the motion mapping between hand gesture and surgical instrument is described by the following equations. For controlling the position of the teleoperated tooltip, (φ, ϕ, d),

$$\varphi[k] = \varphi[k-1] + \tan^{-1}(s_x[k]\Delta p_x[k]), \quad (1)$$

$$\phi[k] = \phi[k-1] + \tan^{-1}(s_z[k]\Delta p_z[k]), \quad (2)$$

$$d[k] = d[k-1] + s_y[k]\Delta\theta_{wrist}[k], \quad (3)$$

where θ_{wrist} is the wrist angle. $[p_x\ p_y\ p_z]^{\text{T}}$ indicates the user's wrist position. $[s_x\ s_y\ s_z]^{\text{T}}$ represents the scaling factor

$$s_x[k] = \frac{k_x|\Delta p_x[k]|}{L_{arm}}, \quad (4)$$

$$s_y[k] = \frac{k_y|\Delta\theta_{wrist}[k]|}{L_{arm}}, \quad (5)$$

$$s_z[k] = \frac{k_z|\Delta p_z[k]|}{L_{arm}}. \quad (6)$$

where k_x, k_y, and k_z is determined as 4.2, 2.0, and 3.5 after experimental tuning and testing process, respectively.

IV. Experimental Results

A series of experiment has been performed to validated the performance of the proposed advanced control interface. The experimental setup, comparisons, and discussions will be described sequentially.

A. System Setup

1) System integration

Three personal computers (PCs) are integrated in the proposed teleoperating surgical system (Fig. 6). The visualization PC (Intel i7-8700 3.2GHz CPU and NVIDIA GeForce GTX 1080 Ti GPU with Windows 10 64-bit) is installed with the stereo camera (ZED mini, Stereolabs, San Francisco, CA) and 3D hologram display (Looking Glass 8.9", Looking Glass Factory, Brooklyn, NY) to provide the user real-time 3D visual feedback. A host PC (Intel i7-8700 3.2GHz CPU with Windows 10 64-bit) is installed with the hand gesture tracker (Leap Motion Controller, Ultraleap, Mountain View, CA) to detect the user's hand gesture and then convert it into motion commands sent to the slave robotic manipulator (LapaRobot). The LapaRobot is controlled by a local target PC (Intel i7-3770 CPU with LabVIEW Real-Time 2018) which receives the motion commands via the UDP protocol and performs closed-loop control on each joint of the LapaRobot. As shown in Fig. 6, the hologram display and hand gesture tracker are presented on the master side. The robot and stereo camera are installed on the slave side.

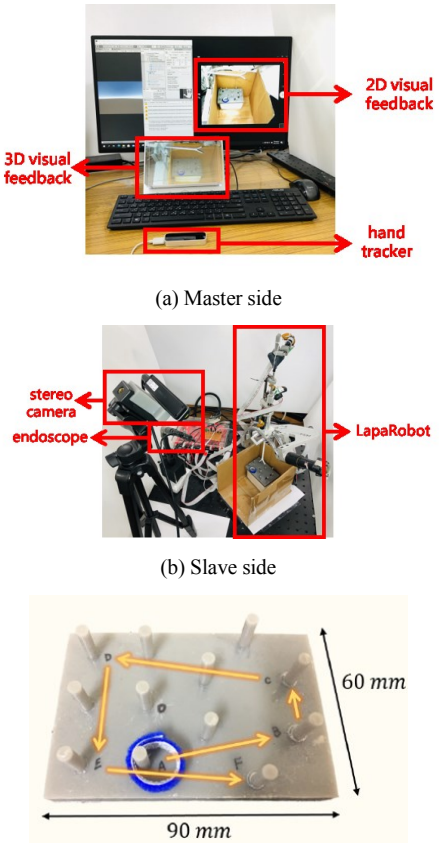

(a) Master side

(b) Slave side

(c) Ring transfer task

Fig. 6. Experimental setup

2) Viewpoint alignment

Even if we possess 3D visualization in the teleoperation system, we still need to correct the perspective of the point cloud and move the key part of it to the center of the display. Wrong viewing angle may lead to users' discomfort or even distract their attention. The problem of askew point cloud mainly results in a tilting camera angle and a lack of object tracking. We do not have a clue to improve it. Hence, we come up with an idea to paste markers on the tool and combine the marker detection data with camera IMU data. Provided with tool position and the camera tilting angles, we adjust the position and rotation of point cloud object in framing volume accordingly. By doing so, surgeons get a better understanding of the surgical site.

B. Arm Length Estimation

In this experiment, the hand gesture tracker is fixed on the table. Five participants are asked to follow the steps written on Unity GUI to perform arm length estimation. Users are allowed to choose right or left-hand mode according to their preference. Before the procedure, we should ensure where the wrist point position, called from Unity Module provided by Ultraleap, is actually located. After the test, we are sure that the wrist position is located at the intersection between the palm print beside the radius bone and the deepest line on the wrist. The actual length of the arm is measured from the wrist point to the olecranon that touches the table using a ruler.

Tables I and II summarizes the experimental results. We find that participants should comply with the instructions below during the initialization procedure to get a better estimation of arm length:

- Participants' wrist need to draw over sphere surface as large as possible.
- Participants should not bend their wrists.
- Participants should open their hand palms.

The estimation errors listed in Table II are all better than the ones listed in Table I. Particularly, all the errors listed in Table II are less than 3%. This result demonstrates the effectiveness of the proposed method.

TABLE I
RESULTS OF ARM LENGTH ESTIMATION WITHOUT INSTRUCTIONS.

Subject	Actual [cm]	Estimated [cm]	Error [%]	Variance [cm^2]
1	27.00	20.68	-23.40	1.59
2	27.70	22.81	-17.66	0.88
3	28.70	22.61	-21.21	1.57
4	26.90	20.79	-22.70	3.44
5	26.20	20.04	-23.51	1.74

TABLE II
RESULTS OF ARM LENGTH ESTIMATION WITH INSTRUCTIONS.

Subject	Actual [cm]	Estimated [cm]	Error [%]	Variance [cm^2]
1	27.00	26.81	-0.72	0.32
2	27.70	27.52	-0.63	0.27
3	28.70	28.47	-0.79	0.23
4	26.90	26.20	-2.60	0.38
5	26.20	26.14	-0.24	0.19

C. *Performance Comparison*

As a fundamental task in laparoscopic surgery training, the ring transfer task involves the long-range transfer and operating precision. By performing this task (Fig. 6(c)), we want to verify the efficacy of the proposed motion mapping method in arm fatigue elimination and evaluate the improvement of operation precision after naked-eye 3D visualization is provided.

The experiment is divided into two parts: (1) comparison of various mapping methods and (2) comparison between 2D and 3D displays. For each part, five participants, same in arm length estimation, are asked to perform the following steps:

- The initial position of the surgical tool-end is right above the peg O with the blue ring placed onto the peg A.
- Participants should control the slave robot and transfer the ring from peg A to B, C, D, E, and F sequentially.
- The task completion time is counted from the moment arm length estimation begins to the moment the ring is placed onto the peg F, and the forceps is released.
- Participants are asked to answer several questions in the questionnaire.
- Repeat the procedure mentioned above five times.

The experimental results and performance comparisons are given as follows.

1) *Comparison of various mapping methods*

The experimental comparison between the traditional and proposed motion mapping is illustrated in Fig. 7. The proposed motion mapping method reduces master path length (see Fig. 7a). Because participants are allowed to rest their elbows on the table, they only have to wave their arms to control the tool translation in the xz-plane. Besides, they wave their palms rather than move their hands up and down to perform tool insertion. Both reasons mentioned above effectively reduce the hand path and eliminate users' physical fatigue at the same time. Subject 4 even reduces the path length up to 50% of the original one.

Both motion mapping methods match their performances in task completion time and the number of ring drop as shown in Fig. 7b and 7c. Ring drop is mainly caused by loss of hand tracking and finger recognition mismatch. Apart from this, we do not mark the standard deviation in the chart of ring drop since the quantitative of it is too little, and the standard deviation lines may mess the chart. Based on the result, we can infer that the performance of task completion time and the number of ring drops are in accordance with how much the participants ease into the jobs. If they get used to the proposed mapping method, we can see significant improvement in the performance and vice versa.

Based on Fig. 7d, the proposed motion mapping method leads to more clutching. Users clutch the system when their hands reach the edges of their motion range. By doing so, the system stops accepting robot commands and pauses the robot. Users can adjust their hand positions to more comfortable zones in this condition, and they can go back to the task mode again. Due to the restricted motion range of arms with elbows placed on the table, it is reasonable to adjust master positions for more times in the proposed motion mapping method. In our system design, the user just has to press several keyboard buttons to change the system state, so more clutching might not seriously impact the task performance.

2) *Comparison between 2D and 3D displays*

The experimental comparison between using the 2D and 3D visual feedback is demonstrated in Fig. 8. 3D vision contributes to fewer collisions and less system clutching during operation as shown in Figs. 8a and 8b. Note that we do not mark the standard deviation in the chart of collisions since the quantitative of it is too little, and the standard deviation lines may mess the chart. With more accurate depth information, participants can avoid unnecessary hand routes and prevent their arms from waving out of the motion range. Thus, the number of clutches decreases. With more sufficient human perceptual cues, the 3D vision diminishes collisions between the surgical tool and the pegboard as well. The advantages mentioned above improve the system's safety and surgical efficiency.

The naked-eye 3D visualization reduces master path length greatly, as shown in Fig. 8c. That is due to that 3D vision effectively avoids depth miscalculation during operation. Participants do not have to adjust the tool position back and forth, leading to shorter path length. Participants eliminate their arm fatigue problem owing to this. In addition, from decreasing the standard deviation between tasks, we can deduce that the 3D vision even makes the system more stable.

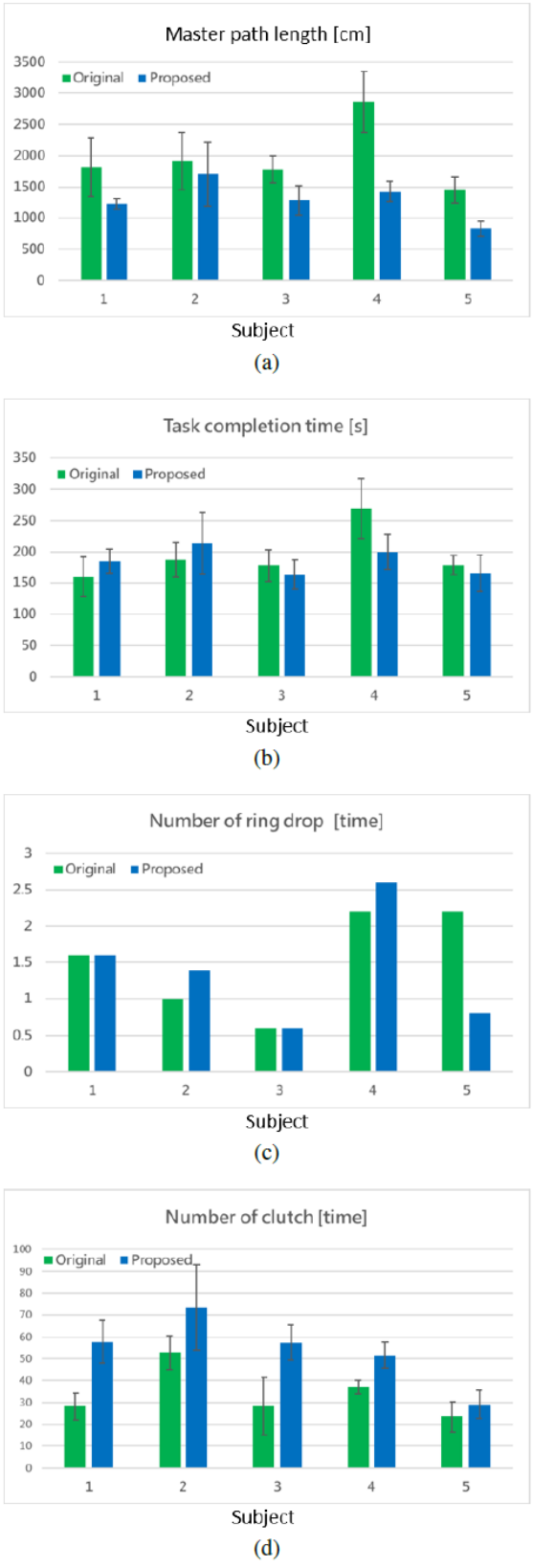

Fig. 7. Experimental comparison between the traditional (green) and proposed (blue) motion mapping. (a) Master path length. (b) Task completion time. (c) Number of ring drop. (d) Number of clutch.

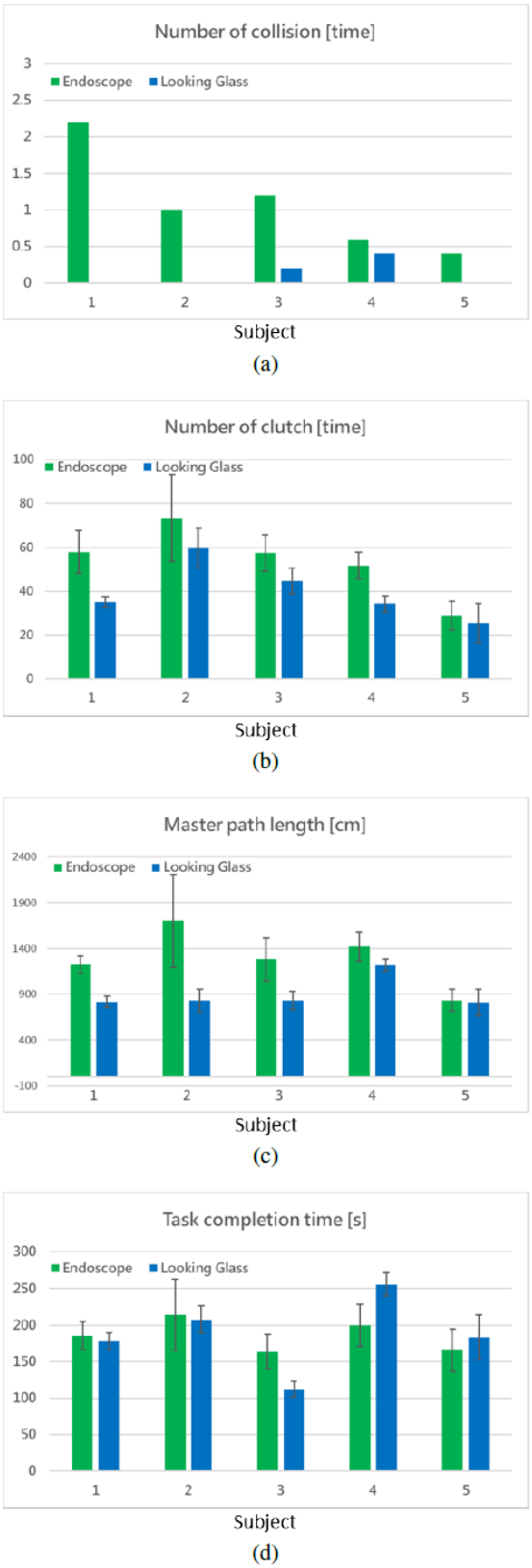

Fig. 8. Experimental comparison between the 2D (green) and 3D (blue) visual feedback. (a) Number of collision. (b) Number of clutch. (c) Master path length. (d) Task completion time.

As for the task completion time (see Fig. 8d), we initially

expect that performing under 3D vision is supposed to take participants more time due to point cloud construction delay. Participants have to wait for the time delay to plan and perform subsequent steps. However, from Fig. 8d, we can find that only Subject 4 and 5 spend more time performing tasks with 3D vision. Therefore, we can state that naked-eye 3D visualization can effectively enhance surgical efficiency after speeding point cloud construction.

3) User experiences

There are two questions listed in the questionnaire. First, scale from 0 to 10, how does the proposed motion mapping method help mitigate the arms fatigue problem for participants. As shown in Fig. 9a, no matter what types of surgical vision are provided, all participants give feedback above seven. We can conclude that the proposed motion mapping method solves the arms fatigue problem of gesture-based interfaces.

Second, scale from 0 to 10, how does the naked-eye 3D visualization help perform ring transfer tasks for participants. From Fig. 9b, we can see that Subject 5 gives feedback of five, a neutral point of view. As far as people with poor spatial awareness or people not used to 3D vision are concerned, they do not like to perform tasks in 3D space; thus, 3D vision does not do much for them. It maybe still needs some training to get people accustomed to 3D applications. After that, 3D vision may greatly improve task performance.

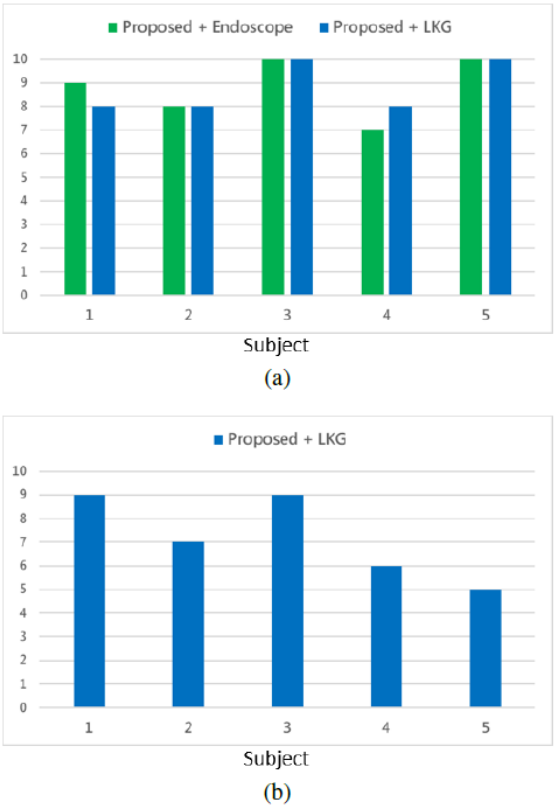

Fig. 9. Results of the user experience questionnaire. (a) Proposed motion mapping mitigates arm fatigue problem. (b) Naked-eye 3D visualization facilitates the operation of ring transfer.

V. Conclusion

This work proposes a hand-robot motion mapping method and a naked-eye 3D visualization framework in the teleoperation system. The motion mapping method allows surgeons to place their elbows on the table during operation. This design effectively eliminates users' arm fatigue issues, which are often arisen when applying gesture-based control interface. Besides, the integrated naked-eye 3D visualization provides surgeons with adequate depth information without discomfort symptoms, such as headaches and nausea. It prevents surgeons from depth miscalculation and promises better path planning and fewer collisions in the task. The future work includes reducing time delay caused by point cloud reconstruction so that users can enjoy 3D surgical vision without waiting for visual feedback synchronization. The finger recognition algorithm will be improved to avoid unexpected interferences during the teleoperation.

Acknowledgment

The content of this work has mostly been reported in Mr. Chung-Chun Wang's master's thesis. The authors would like to thank Prof. Chung-Hsien Kuo, the President of Robotics Society of Taiwan (RST), for his invitation and encouragement to publish this work on the *International Journal of iRobotics*.

References

[1] S. Avgousti, E. G. Christoforou, A. S. Panayides, S. Voskarides, C. Novales, L. Nouaille, C. S. Pattichis, and P. Vieyres, "Medical telerobotic systems: current status and future trends," *Biomedical engineering online*, vol. 15, no. 1, pp. 1–44, 2016.

[2] A. Trejos, R. Patel, I. Ross, and B. Kiaii, "Optimizing port placement for robot-assisted minimally invasive cardiac surgery," *The International Journal of Medical Robotics and Computer Assisted Surgery*, vol. 3, no. 4, pp. 355–364, 2007.

[3] X. Zhang, Z. Wei, M. Bie, X. Peng, and C. Chen, "Robot-assisted versus laparoscopic-assisted surgery for colorectal cancer: a meta-analysis," *Surgical endoscopy*, vol. 30, no. 12, pp. 5601–5614, 2016.

[4] T. A. Lawrie, H. Liu, D. Lu, T. Dowswell, H. Song, L. Wang, and G. Shi, "Robot-assisted surgery in gynaecology," *Cochrane Database of Systematic Reviews*, no. 4, 2019.

[5] M. C. B. Seixas, J. C. Cardoso, and M. T. G. Dias, "The leap motion movement for 2d pointing tasks: Characterisation and comparison to other devices," in *2015 International Conference on Pervasive and Embedded Computing and Communication Systems (PECCS)*. IEEE, 2015, pp. 15–24.

[6] H. Ren, W. Liu, and A. Lim, "Marker-based surgical instrument tracking using dual kinect sensors," *IEEE transactions on automation science and engineering*, vol. 11, no. 3, pp. 921–924, 2013.

[7] S. W. Prince, C. Kang, J. Simonelli, Y.-H. Lee, M. J. Gerber, C. Lim, K. Chu, E. P. Dutson, and T.-C. Tsao, "A robotic system for telementoring and training in laparoscopic surgery," *The International Journal of Medical Robotics and Computer Assisted Surgery*, vol. 16, no. 2, p. e2040, 2020.

[8] C. Cao, C. L. MacKenzie, and S. Payandeh, "Task and motion analyses in endoscopic surgery," in *Proceedings ASME Dynamic Systems and Control Division. Citeseer*, 1996, pp. 583–590.

[9] J. Yuan, B. Mansouri, J. H. Pettey, S. F. Ahmed, and S. K. Khaderi, "The visual effects associated with head-mounted displays," *Int J Ophthalmol Clin Res*, vol. 5, no. 2, p. 085, 2018.

[10] H. Spath, "Least-square fitting with spheres," *Journal of optimization theory and applications*, vol. 96, no. 1, pp. 191–199, 1998.

Chung-Chun Wang received the M.S. degree in Electrical Engineering from National Taiwan University in 2021. His current research interests and publications are in the areas of control and robotics.

Cheng-Wei Chen received the Ph.D. degree in mechanical engineering from the University of California, Los Angeles, in 2018. He is currently an associate professor in electrical engineering, National Taiwan University, Taipei, Taiwan. His research interests include robotics, mechatronics, digital control systems, and numerical optimization**.**